Filamentation instability of a fast electron beam in a dielectric target

A. Debayle and V. T. Tikhonchuk
Centre Lasers Intenses et Applications, Université Bordeaux 1, CNRS, CEA, 351, Cours de la Libération, 33405 Talence Cedex, France
(Received 31 July 2008; revised manuscript received 16 October 2008; published 12 December 2008)

High-intensity laser-matter interaction is an efficient method for high-current relativistic electron beam production. At current densities exceeding a several kA μm^{-2}, the beam propagation is maintained by an almost complete current neutralization by the target electrons. In such a geometry of two oppositely directed flows, beam instabilities can develop, depending on the target and the beam parameters. The present paper proposes an analytical description of the filamentation instability of an electron beam propagating through an insulator target. It is shown that the collisionless and resistive instabilities enter into competition with the ionization instability. This latter process is dominant in insulator targets where the field ionization by the fast beam provides free electrons for the neutralization current.

DOI: 10.1103/PhysRevE.78.066404 PACS number(s): 52.35.−g, 52.40.Mj, 52.59.−f, 52.57.Kk

I. INTRODUCTION

The laser is becoming an efficient tool for acceleration of electrons and ions to high energies. This new technique could be more efficient and less cumbersome than conventional accelerators. Many applications of laser-accelerated particles can be found spreading from medicine to fast ignition in inertial confinement fusion (ICF). In the medical applications, the electron or ion beams are used to reach and to destroy a tumor without damaging a significant number of healthy cells. In the ICF case, the electron (or ion) beam has to transport the laser energy from critical density to the high-density core to ignite the deuterium-tritium fuel. Moreover, the ion beams can be produced in the sheath electric field generated by the electron beam. Thus, a reliable control of all the electron beam parameters is needed, i.e., the density, the divergence, and the energy spectrum of the beam.

A high-density current can be easily destroyed by self-consistent electric and magnetic fields in vacuum. However, it can propagate a long distance in a dense target if a neutralization current of target electrons is created by the longitudinal electric field of the incident beam. In metals, the neutralization current is set up by the free electrons in the time scale $\tau=\varepsilon_0/\sigma\sim 0.1$ fs, where σ is the electrical conductivity and ε_0 is the void permittivity. In insulator targets, ionization is needed to provide the electrons for the return current. This effect considerably increases the neutralization time ($\tau\gtrsim 1$ fs) and the target resistivity.

Concerning the propagation of the fast electrons, experiments with metal targets have shown a homogeneous and stable beam penetration through the solids [1–4]. In plastic targets, despite the fact that the penetration depth is comparable with that of metals, the beam becomes filamented after a propagation of several tens of micrometers [4–9]. The origin of this filamentation has not clearly been identified yet, since it can be related to the Weibel instability, or the resistive instability, or the ionization instability. This last has been recently suggested for explanation of the experimental results in [5] and is based on an analytical model developed quantitatively for high wave numbers [10]. The instability finds its origin in the dependence of the local beam velocity on the local beam density.

We propose an analytical model for the ionization instability in a more general case, taking into account the magnetic field, the fast electron kinetics, and the collisional ionization of atoms by the plasma electrons. It is based on a previous work describing the propagation of fast electrons through dielectric targets [11] and allows us to consider the filamentation and ionization instabilities within the same formalism. The article is developed as follows. Section II presents a brief recall of the one-dimensional (1D) stationary beam propagation model developed in [11] and validated in [12]. It describes the background state and the main physical assumptions. The instability description is presented in Sec. III. It considers the limit of small wave numbers, where the perturbation wavelength is larger than the ionization front thickness. The relative role of electric and magnetic fields is analyzed and two limits of the resistive and field ionization instabilities are discussed. The main results are summarized in the Conclusion.

II. STATIONARY BEAM PROPAGATION MODEL: RECALL

The relativistic electrons are supposed to be collisionless. The beam can be divided into two main parts: the head and the body. In the beam head, the fast electrons evolve in a neutral matter and generate an electric field sufficient to ionize a part of the atoms. The newly created electrons, accelerated in the opposite direction, create a return current. In the beam body, the electric field ionization stops and it is followed by a collisional ionization of atoms by the thermal plasma electrons. This ionization is controlled by the plasma heating due to the highly collisional return current. Figure 1 presents a schematic view of the beam characteristics, supposing their variation in one dimension along the propagation direction.

Approximate solutions can be found by assuming a constant beam velocity v_f, which implies that beam energy losses are small. In the reference frame related to the ionization front, the propagation process is stationary. In the laboratory reference frame, the fast electrons enter the front with the initial velocity v_{b0}^{+} higher than the front velocity v_f, and slow down there by creating an electric field. They leave the

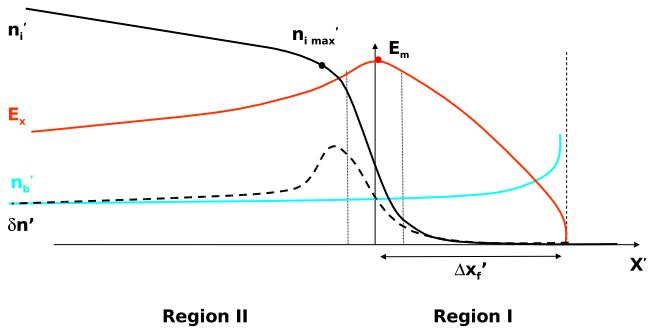

FIG. 1. (Color online) Qualitative profiles of the longitudinal electric field E_x, the ion density n_i', the beam density n_b', and the charge separation $n_i'-n_e'=\delta n'$ in the front reference frame centered around the electric field maximum E_m. The zone I, of thickness $\Delta x_f'$, corresponds to the beam head where occurs the fast charge accumulation and the electric field ionization. The zone II corresponds to the beam body where occurs the collisional ionization. $n_{i\,\max}$ is the ion density after the electric field ionization.

front with velocity v_{b0}^- lower than the beam velocity. In what follows we suppose that the difference $|v_{b0}^{\pm}-v_f| \ll c$ is small, that is, the beam is nonrelativistic in the front reference frame.

A. Basic set of equations

Let us consider a monoenergetic beam of fast electrons propagating in the positive x direction with an initial density n_{b0}, initial energy $\epsilon_{b0}=mc^2(\gamma_{b0}-1)$, and the relativistic factor $\gamma_{b0}=(1-v_{b0}^2/c^2)^{-1/2}$, in the laboratory reference frame. The ionization front structure can be better described in the front reference frame (marked with a prime in what follows). In the beam head, region I in Fig. 1, the negative charge accumulation $-e(n_b'^{+}+n_b'^{-})$ increases the longitudinal electric field E_x according to the Poisson equationn

$$\varepsilon_0 \frac{dE_x}{dx'} = e(\Delta n' - n_b'), \tag{1}$$

where $\Delta n'=n_i'-n_e'$ is the charge density, n_i' is the ion density, n_e' is the plasma electron density and $n_b'=n_b'^{+}+n_b'^{-}$ is the total fast electron density in the front, including the entering and the reflected electrons. The polarization term that described the ionization losses is neglected as we are interested here in sufficiently weak beam currents [11]. The fast electron kinetics is described by the current conservation and the momentum conservation equations:

$$m_e v_b'^{\pm}\frac{dv_b'^{\pm}}{dx'} = -eE_x, \quad n_b'^{\pm}v_b'^{\pm} = \pm n_{b0}'v_{b0}'. \tag{2}$$

The charge accumulation occurs on a short length $\Delta x_f' \sim 1\ \mu$m. The electric field rises above the threshold and it ionizes atoms in the tunnel regime in a thin region $\Delta x_i' \ll \Delta x_f'$. These newly created electrons are accelerated backward and create the return current. This process is described by the following set of equations:

$$v_e'' = -\frac{eE_x}{m_e \nu_e \gamma_f^2}, \tag{3}$$

$$\frac{d[n_e'(v_e''-v_f)]}{dx'} = -v_f\frac{dn_i'}{dx'} = \nu_a n_a \frac{E_a}{E_x} e^{-2E_a/3E_x}. \tag{4}$$

Here, n_a is the density of neutral atoms, $\nu_a=12v_a J_a/a_B J_h$ is the characteristic bound electron frequency, $v_a=e^2/4\pi\varepsilon_0\hbar$ is the characteristic bound electron velocity, $a_B=4\pi\varepsilon_0\hbar^2/m_e e^2$ is the Bohr radius, $E_a=(e/4\pi\varepsilon_0 a_B^2)(J_a/J_h)^{3/2}$ is the atomic field, $\gamma_f=(1-v_f^2/c^2)^{-1/2}$ is the Lorentz factor of the front reference frame, and J_a and J_h are the atom ionization potential and the hydrogen ionization potential, respectively. The plasma electron inertia is neglected in Eq. (3), since the electron collision time $1/\nu_e \sim 1$ fs is supposed to be much shorter than the characteristic time of electron beam evolution. According the relativistic velocity transformation, the electron drift velocity in the laboratory reference frame, $v_e=-eE_x/m_e\nu_e$, becomes $v_e' \approx -v_f+v_e''$ with $v_e'' \approx v_e/\gamma_f^2$ in the front reference frame.

After the zone of tunnel ionization, the plasma charge separation $\Delta n'=n_i'-n_e'>n_b'$ screens the electric field created by the beam electrons. The electric field ionization is followed by the plasma electron heating and the secondary collisional ionization. This process is described by the following set of equations:

$$\frac{d[n_e'(v_e''-v_f)]}{dx'} = -v_f\frac{dn_i'}{dx'} = W_{ea}n_i(n_a-n_i), \tag{5}$$

$$-v_f\frac{3}{2}\frac{d(n_e'T_e)}{dx'} = j_e E_x + v_f \alpha J_a \frac{dn_i'}{dx'}, \tag{6}$$

where $j_e=-en_e v_e$ is the plasma electron current density, and $W_{ea} \simeq 6a_B^2 v_a (T_e/J_a)^{1/2} e^{-J_a/T_e}$ [13] is the collisional ionization rate, averaged over a Maxwellian distribution. The electron-electron-ion recombination rate is neglected because of the high electron plasma temperature $T_e \sim J_a$ [11]. The Ohmic heating $j_e E_x$ increases the plasma electron temperature T_e, while the collisional ionization of the atoms reduces the total heating rate. The factor $\alpha \sim 2$ accounts for the excitation of atoms.

B. Beam structure in the 1D model

The self-generated electric field by the negative charge accumulation in the beam head slows down the fast electrons as long as the ionization has not been started ($\Delta n'=0$). The relation between the local electron density n_b' and the electric potential $-d\varphi'/dx'=E_x$ follows from the fast electron equations (2): $n_b'(\varphi')=2n_{b0}'(1+e\varphi'/\varepsilon_{b0}')^{-1/2}$, where $\varepsilon_{b0}'=\gamma_f(\varepsilon_{b0}+m_e c^2-v_f p_{b0})-m_e c^2$ is the fast electron energy in the front reference frame and $p_{b0}=m_e\gamma_{b0}v_{b0}$ is the fast electron momentum.

The maximum electric field E_m in the charge accumulation zone and the ionization level $n_{i\,\max}'$ follow from Eqs. (1) and (4) integrated over the beam front thickness $\Delta x_f'$ (see Fig. 1):

$$E_m^2 = E_a^2 \frac{n_{b0}}{n_{cE}}\frac{v_{b0}'^2}{2c^2\gamma_f}, \tag{7}$$

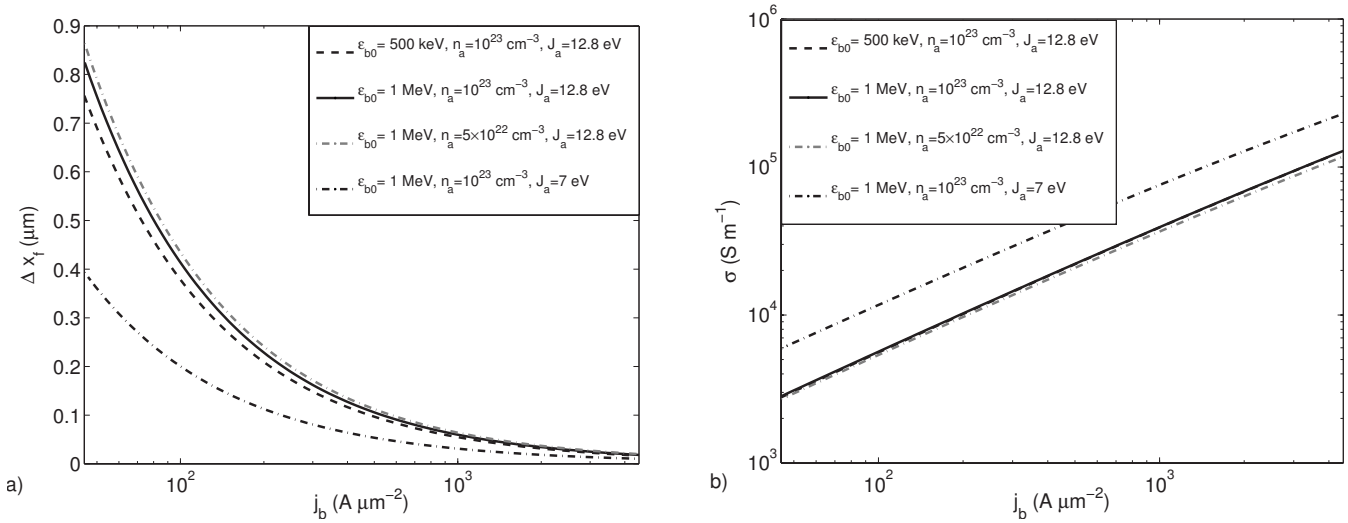

FIG. 2. Dependence of the front thickness (a), and the plasma conductivity behind the ionization front (b) on the beam current for different beam energies and target parameters. The elastic collision frequency of plasma electrons is set to $\nu_e = 1$ fs^{-1}.

$$n'_{i\,\max} = 2\sqrt{3\pi m_e \varepsilon_0 \nu_a \nu_e n_a \gamma_f^2/4e^2} e^{-E_a/3E_m}. \tag{8}$$

Equation (7) describes the energy conversion of fast electrons in the electrostatic field. The characteristic beam density $n_{cE} = \varepsilon_0 E_a^2/8m_e c^2$ required to reach the electric ionization level is approximately 5×10^{18} cm^{-3}. In order to close the system and to find the front velocity v_f, one needs a third equation, which comes from the charge neutralization: The electric field achieves its maximum in the point where the negative charge accumulation in the front is balanced by the positive plasma charge separation $\Delta n' \approx v''_e n'_i / v_f$ deduced from Eq. (4). Then, according to the Poisson equation (1), the ion density at the electric field maximum reads

$$n'_{i\,\max} \approx -4n'_{b0} \frac{v_f}{v''_e(E_m)} = n_{b0} \frac{4\gamma_f m_e \nu_e v_f}{eE_m}. \tag{9}$$

This relation (9) is equivalent to the current neutralization in the laboratory reference frame, that is, $n_i v_e = 2n_{b0} v_f$. The solution of the system of equations (7)–(9) provides the formulas for the front velocity, the ionization level, and the electric field maximum depending on the beam energy and density. Asymptotically, one finds

$$\beta_f = \beta_{b0} - \sqrt{\frac{2n_{cE}}{\gamma_{b0}^3 n_{b0}}} \frac{1}{3|\ln \Lambda|}, \tag{10}$$

$$E_m = \frac{1}{3} E_a |\ln \Lambda|^{-1} \sim (0.04 - 0.1) E_a, \tag{11}$$

where $\Lambda = \beta_{b0} \sqrt{6\nu_e n_{b0}^2 / \pi \nu_a n_{cE} n_a} \ll 1$, $\beta_f = v_f/c$, and $\beta_{b0} = v_{b0}/c$.

The front velocity increases with the beam density. The characteristic parameter is the dimensionless derivative $D = d \ln v_f / d \ln n_{b0}$:

$$D \approx \frac{1}{\beta_{b0}} \sqrt{\frac{2n_{cE}}{\gamma_{b0}^3 n_{b0}}} \left(\frac{1}{2} - \frac{1}{|\ln \Lambda|} \right). \tag{12}$$

It is a small parameter, $D \sim 10^{-2}$, and it is inversely proportional to the square root of the beam current density. It does not depend on the target density, and increases with the mean ionization potential as $D \propto J_a^{3/2}$. For high beam densities, v_f is close to v_{b0}, and D becomes very small.

Our theory supposes that the beam density is small compared to the plasma electron density. According to Eq. (9), $n_{b0}/n_{i\,\max} = v_e(E_m)/4v_f \sim 10^{-2} - 10^{-3}$. Therefore, the assumption of weak ionization in the front is verified as long as $j_{b0} \ll e v_{b0} n_a v_e(E_m)/v_f \sim 40$ kA μm^{-2}. The electron beam velocity in the front reference frame is written

$$\frac{v'_{b0}}{v_f} \approx \gamma_{b0}^2 (\beta_{b0} - \beta_f) \approx |\ln \Lambda|^{-1} \sqrt{2\gamma_{b0} \frac{n_{cE}}{n_{b0}}}. \tag{13}$$

Thus, the nonrelativistic approximation $v'_{b0}/v_f \ll 1$ is valid as long as $j_{b0} \gg 0.03 e n_{cE} v_{b0} \gamma_{b0}$. For a 1 MeV beam, the minimum beam current density is a few A μm^{-2}.

Knowing the beam density n'_b, one can estimate the front thickness $\Delta x'_f$ from the Poisson equation (1). Neglecting the charge separation term $\Delta n'$ and integrating (1) along the front thickness, one finds

$$\Delta x'_f = \frac{\varepsilon_0 E_m \gamma_f}{6e n_{b0}}. \tag{14}$$

The front thickness expressed in the laboratory reference frame, $\Delta x_f = \Delta x'_f / \gamma_f$, is plotted in Fig. 2(a). It is smaller than 1 μm and it decreases with the beam density. It is strongly sensitive to the mean ionization energy, $\Delta x_f \propto J_a^{3/2}$, as for a lower ionization energy, the ionization probability is higher and, consequently, the charge accumulation thickness smaller. The newly created electrons, which have a mean energy of several eV, are highly collisional. The collisional ionization follows the electric field ionization (see region II in Fig. 1). This process is described by Eqs. (5) and (6),

assuming the current neutralization $j_b=-j_e$ with $j_b=-2en_{b0}v_f$. This hypothesis is reasonable as the neutralization distance is small compared with the beam length. According to Eq. (1), the neutralization length $l_s=\varepsilon_0 m_e\nu_e\gamma_f^2 v_f/e^2 n'_{i\,\max}$ is of the order of a few micrometers for a low beam density $n_{b0}\sim 10^{18}$ cm^{-3}. Behind the ionization front, the electric field tends to the resistive electric field limit, $E_r=E_m/2$.

As the ionization is initialized by the electric field, the plasma electrons are not in a local thermodynamic equilibrium with the atoms and ions. Their temperature is too high compared with the ionization level. All the energy deposited by Ohmic heating is converted into the ionization, and the temperature remains approximately constant. Thus the plasma electron energy equation (6) simplifies to

$$\frac{1}{n'_i}\frac{dn'_i}{dx'}=-\frac{1}{L_0}\frac{n'^2_{i\,\max}}{n'^2_i}, \tag{15}$$

where $L_0=e^2v_f\alpha J_a n'^2_{i\,\max}/m_e\nu_e j_b^2\gamma_f$ is the characteristic ionization length. As the fast electrons slowly lose their energy, the current density j_b is approximately constant and the plasma density is written

$$n_{i0}(x')=n'_{i\,\max}\sqrt{1+2x'/L_0}. \tag{16}$$

This ionization regime occurs as long as the recombination is weak. The conductivity just after the ionization front is written $\sigma_{\min}=e^2n_{i\,\max}/m_e\nu_e$. It is typically a hundred times lower than in metals [see Fig. 2(b)] and it does not depend on the beam energy and the target density.

III. IONIZATION INSTABILITY

The electric field ionization results in increasing front velocity with the beam density. This dependence could create a front rippling, if the fast electron current is amplified in regions where the density is higher. Therefore, the main challenge lies in describing the processes that deflect fast electrons toward the high local beam density regions. Two cases are considered below. For a perturbation that grows with a characteristic time large compared with the time of electron crossing the amplification length (Sec. III B), the electromagnetic field coupling can be neglected and the fast electron beam current is neutralized. The fast electrons are accumulated by the electrostatic field, which is itself created by the return current. For a faster-growing instability (Sec. III C), the electromagnetic field coupling is dominant and the hypothesis of a complete beam neutralization is no longer valid. In the laboratory reference frame, the fast electrons are deflected by the self-consistent magnetic field, which is generated by the net current.

A. Basic set of equations

Let us assume that the electric field ionization region is a thin interface $\zeta(y,t')$ centered at $x'=\langle\zeta(y,t')\rangle=0$. The thickness of the ionization region $\Delta x'_f$ is supposed to be much smaller than the front perturbation wavelength $\lambda=2\pi/k_y$. Behind the beam front, the fast electrons evolve in a plasma where the collisional ionization of atoms by the plasma electrons is the dominant process.

The transport equations are written in a two-dimensional geometry. The stationary 1D solutions are presented in Sec. II, and the 2D equations are linearized by introducing a perturbation for each quantity along the transverse direction y such as $A(x',y,t')=A_0(x')+\delta A(x')e^{-i\omega' t'+ik_y y}$. Then the fast electrons satisfy the following equations:

$$-i\omega'\delta n'^{\pm}_b\pm v'_{b0}\frac{d\delta n'^{\pm}_b}{dx'}+n'_{b0}\left(\frac{d\delta v'^{\pm}_{bx}}{dx'}+ik_y\delta v'^{\pm}_{by}\right)=0, \tag{17}$$

$$-i\omega'\delta v'^{\pm}_{bx}\pm v'_{b0}\frac{d\delta v'^{\pm}_{bx}}{dx'}=-\frac{e}{m_e}\delta E_x, \tag{18}$$

$$-i\omega'\delta v'^{\pm}_{by}\pm v'_{b0}\frac{d\delta v'^{\pm}_{b}}{dx'}=-\frac{e}{m_e}\delta E'_y. \tag{19}$$

The fast electron deflection by the magnetic field is neglected since they are not relativistic in the front reference frame. Concerning the Maxwell's equations for the electric and magnetic fields, several simplifications can be made. First, we are interested in perturbations with the wavelength much longer than the Debye length. Then, the Poisson equation reduces to the charge neutrality condition

$$\delta\Delta n'=\delta n'^{+}_b+\delta n'^{-}_b, \tag{20}$$

where $\delta\Delta n'=\delta n'_i-\delta n'_e$. Moreover, considering low-frequency perturbations, $|\omega'|\ll k_y c$, the displacement current can be neglected in the Ampère equation. Then the perturbations of electric and magnetic field are described by two equations:

$$\frac{d\delta E'_y}{dx'}-ik_y\delta E_x=i\omega'\delta B'_z, \tag{21}$$

$$-\frac{ik_y}{e\mu_0}\delta B'_z=\delta\Delta n' v_f+n'_{i0}\delta v''_{ex}+\delta n'_i v''_{e0}+n'_{b0}(\delta v'^{+}_{bx}+\delta v'^{-}_{bx}). \tag{22}$$

A part of the beam current density perturbation is neglected in the Ampère equation. Indeed, the charge neutralization (20) implies that $v_f\delta\Delta n'\gg v'_{b0}(\delta n'^{+}_b-\delta n'^{-}_b)$. Another component of the Ampère equation along the y axis is not needed here since the system is closed with the plasma charge continuity equation:

$$-i\omega'\delta\Delta n'-v_f\frac{d\delta\Delta n'}{dx'}=\frac{d}{dx'}(\delta n'_i v''_{e0})+\frac{d}{dx'}(n'_{i0}\delta v''_{ex})+ik_y n'_{i0}\delta v'_{ey}. \tag{23}$$

The temperature perturbation has been neglected since isothermal collisional ionization is assumed. The plasma electron momentum equation in the front reference frame is written

$$\frac{\delta v''_{ex}}{v''_{e0}} \approx \frac{\delta E_x}{E_r}, \quad \frac{\delta v'_{ey}}{v''_{e0}} \approx \gamma_f^2 \frac{\delta E'_y + v_f \delta B'_z}{E_r}, \tag{24}$$

where $E_r = E_m/2$ is the resistive electric field. The plasma electron inertia is neglected since it is supposed that $\nu_e/\gamma_f \gg \omega'$. The friction force acting on electrons is not collinear with their relative velocity with respect to ions in the front reference frame, which has the components $\delta v''_{ex}$ and $\delta v'_{ey}$. This is due to the relativistic transformation of the velocity. Finally, the plasma electron energy equation (6), in the isothermal regime describes the ion density variation due to the collisional ionization:

$$-i\omega' \delta n'_i - v_f \frac{d\delta n'_i}{dx'} = \frac{m_e \nu_e \gamma_f^3}{\alpha J_a}(v''^2_{e0} \delta n'_i + 2v''_{e0} n'_{i0} \delta v''_{ex}) = \frac{n'_{i0} v_f}{L_0}\left(\frac{\delta n'_i}{n'_{i0}} + 2\frac{\delta v''_{ex}}{v''_{e0}}\right). \tag{25}$$

This system of 12 differential equations is completed with the boundary conditions at the interface $x' = \zeta = \zeta_0 \exp[-i\omega' t' + ik_y y]$ and the evanescent conditions at $x' \to -\infty$. A solution to this system will provide a dispersion relation for the eigenfrequency $\omega(k_y)$. The instability occurs if the perturbation increases in time, i.e., Im $\omega' > 0$.

B. Electric-field-driven ionization instability

Let us consider the case where the electrostatic field dominates the instability development assuming an irrotational electric field and a low frequency perturbation, that is, $k_y|\delta E_x| \gg |\omega' \delta B'_z|$. Then, Eq. (21) is written

$$\frac{d\delta E'_y}{dx'} = ik_y \delta E_x. \tag{26}$$

This important assumption will be verified at the end of this section. Using the relations (9) and (15), the equation for the ion density perturbation (25) can be written as

$$\frac{d}{dx'}\frac{\delta n'_i}{n'_i} = -\frac{2}{L_0}\frac{\delta E_x}{E_r}. \tag{27}$$

The plasma charge conservation equation (23) in the quasistatic regime, accounting for the quasineutrality condition (20), reads

$$\frac{d}{dx'}\frac{\delta n'^+_b + \delta n'^-_b}{2n'_{b0}} = \frac{d}{dx'}\frac{\delta n'_i}{n'_{i0}} + \frac{d}{dx'}\frac{\delta E_x}{E_r} + ik_y \gamma_f^2 \frac{\delta E'_y + v_f \delta B'_z}{E_r}. \tag{28}$$

These equations for the perturbed quantities along with Eqs. (17)–(19) for fast electrons can be solved assuming that the collisional ionization length L_0 is much larger than perturbation wavelength $2\pi/k_y$. Then, solutions for the homogeneous system of equations can be presented in the form $\delta A(x') = A \exp(i\int k'_x dx')$, where k'_x are the complex eigenvalues of the system.

The beam velocity perturbations are found from the momentum conservation equations (19):

$$\frac{\delta \mathbf{v}'^{\pm}_b}{v'_{b0}} \approx \pm i\frac{\kappa}{k'_x}\left(1 \pm \frac{\omega'}{k'_x v'_{b0}}\right)\frac{\delta \mathbf{E}'}{E_r}, \tag{29}$$

where the parameter $\kappa = \nu_e \gamma_f^2 |v''_{e0}|/v'^2_{b0} = (3\Delta x'_f)^{-1}$ defines the maximum wave number of the model ($k_y \ll \kappa$). The beam density perturbations follow from Eq. (17) coupled to Eqs. (26) and (29):

$$\frac{\delta n'^{\pm}_b}{n'_{b0}} \approx -i\kappa \frac{k'^2_x + k_y^2}{k'^3_x}\left(1 \pm 2\frac{\omega'}{k'_x v'_{b0}}\right)\frac{\delta E_x}{E_r}. \tag{30}$$

The magnetic field perturbation can be evaluated from the Ampère equation. However, in this case, instead of Eq. (22), it is more appropriate to use the projection of Ampère equation on the y axis:

$$-ik'_x \frac{Q}{\kappa}\frac{v_f \delta B'_z}{E_r} = \frac{\delta v'_{ey}}{v''_{e0}} - \frac{v'_{b0}}{v_f}\frac{\delta v'^+_{by} + \delta v'^-_{by}}{2v'_{b0}}, \tag{31}$$

where $Q = \gamma_f \kappa/\mu_0 \sigma_{\min} v_f$ is the magnetic field screening parameter. The last term related to the fast electron current is small, because $v'_{b0} \ll v_f$, and it can be neglected. Moreover, knowing the expressions for κ and $\sigma_{\min}$, one can show that $Q \sim 1$, and therefore, the term in the left-hand side of Eq. (31) is also small. Then using Eq. (24) we find the magnetic field perturbation

$$v_f \delta B'_z \approx -\delta E'_y\left(1 - i\frac{k'_x Q}{\kappa \gamma_f^2}\right), \tag{32}$$

where the second term in the parentheses in the right-hand side is a small correction. Thus, the magnetic field amplitude, in the front reference frame, is $\delta B'_z \sim -\delta E'_y/v_f$. This result can be readily interpreted in the laboratory reference frame. As the plasma neutrality is assumed, the neutralization time of the beam by the plasma electrons is very short, that is, $\omega \ll \omega_{pe}$ where $\omega_{pe} = \sqrt{e^2 n_e/m_e \varepsilon_0}$ is the plasma frequency. Thus, there is no transverse displacement of the plasma electrons that is, $\delta E_y = 0$. In the front reference frame, this is equivalent to the condition $\delta E'_y = -v_f \delta B'_z$. Moreover, the expression (32) justifies our assumption that the magnetic field does not affect the fast electrons, that is, $v'_{b0} \delta B'_z \ll \delta E'_y$.

Injecting the expressions for the beam velocities (29) and densities (30) in the plasma charge conservation equation (28), one obtains the characteristic equation for the parallel wave number k'_x:

$$(k'^2_x + k_y^2)\frac{\kappa}{k'^2_x} = ik'_x - \frac{2}{L_0} - k_y^2 \frac{Q}{\kappa}. \tag{33}$$

Three terms in the right-hand side account, respectively, for the perturbation of the total beam density due to the longitudinal return current, the collisional ionization, and the transverse component of the return current. This equation has to be solved in the small wave number limit corresponding to the thin front approximation, $k_y \Delta x'_f \ll 1$ i.e., $k_y \ll \kappa$. Moreover, the stationary 1D model is valid if the collisional ionization length is larger than the field ionization front thickness, that is, $L_0 \kappa \gg 1$. This latter condition requires a sufficiently strong current or a low ionization energy of the media:

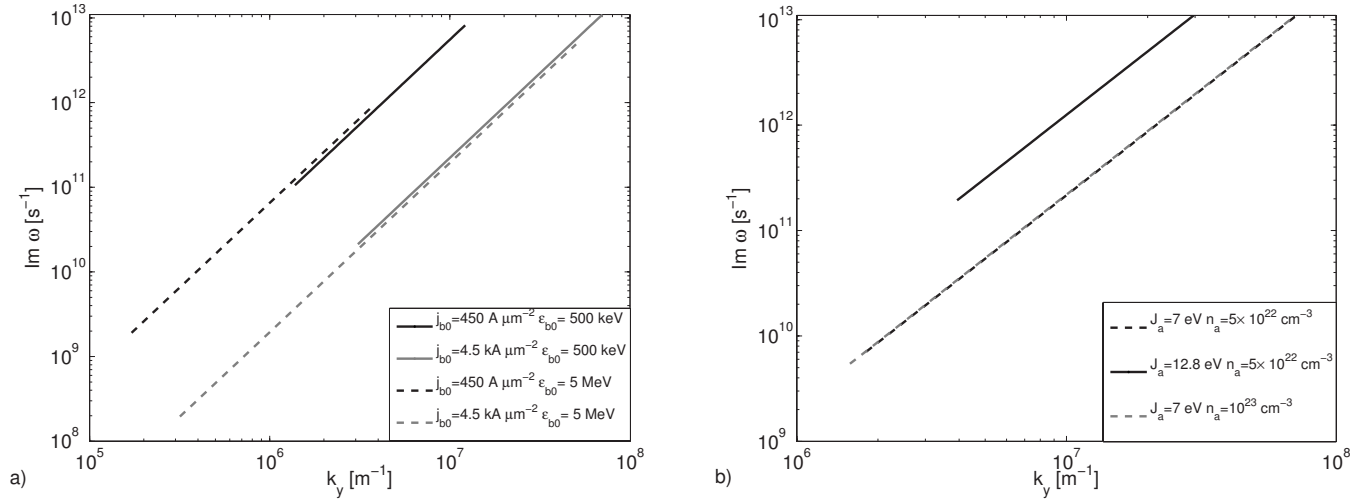

FIG. 3. Dependence of the electrostatic instability growth rate Im ω on the wave number k_y for different beam current densities and beam energies: (a) $\nu_e=1$ fs^{-1}, $n_a=5\times10^{22}$ cm^{-3}, $J_a=7$ eV; (b) $j_b=4.5$ kA μm^{-2}, $\epsilon_b=1$ MeV, and $\nu_e=1$ fs^{-1}.

$$j_{b0} \gg en_{cE}v_{b0}\frac{2eE_ac}{3\nu_eJ_a}|\ln\Lambda|^{-3} \sim \left(\frac{J_a}{J_h}\right)^{7/2} \text{kA } \mu\text{m}^{-2}. \quad (34)$$

The right-hand side of Eq. (33) contains two small parameters $1/L_0\kappa$ and k_y^2Q, which allow us to construct an approximate solution. The dominant term in the left-hand side provides the zero-order solution, $k'_{x0}\approx -ik_y$, where the sign is chosen by the evanescent condition at $x'\to-\infty$. Considering the right-hand side terms as corrections to this solution, one finds

$$k'_x \approx -ik_y - i\frac{k_y^2}{2\kappa} + i\frac{k_y}{L_0\kappa} + i\frac{k_y^3Q}{2\kappa^2}. \quad (35)$$

This solution in the collisional ionization region has to verify the boundary condition at the beam front, $x'=\zeta$, which accounts for the process of electric field ionization. Since we have selected only one eigenvalue k'_x, one boundary condition is sufficient. The front velocity is defined by the fast electrons, which enter and leave the electric field ionization region: $\frac{1}{2}(v_{bx}^+ + v_{bx}^-) = v_f + \delta v_f$. Moreover, the perturbation of the front velocity can be related to the beam density perturbation. Combining these two conditions, and knowing that $\delta v_{bx}'^{\pm} = \delta v_{bx}^{\pm}\gamma_f^2$, according the relativistic velocity transformation, one finds

$$\frac{1}{2}[\delta v_{bx}'^{+}(0) + \delta v_{bx}'^{-}(0)] = \gamma_f^2\delta v_f = \gamma_f^2\frac{dv_f}{dn'_{b0}}[\delta n_b'^{+}(0) + \delta n_b'^{-}(0)]. \quad (36)$$

The fast electron velocity and density perturbations follow from Eqs. (29) and (30). Then Eq. (36) leads to the following dispersion equation:

$$\omega' k'_x = -2v_f\gamma_f^2 D(k_x'^2 + k_y^2), \quad (37)$$

where $k'_x(k_y)$ is defined by Eq. (35). In the low-frequency limit $\omega' \ll k_y v'_{b0}$, the frequency is written

$$\omega' = 4i\gamma_f^2 Dk_y v_f\left(\frac{k_y}{2\kappa} - \frac{1}{L_0\kappa} - \frac{k_y^2Q}{2\kappa^2}\right) \approx 6i\gamma_f^2 Dv_f\Delta x'_f k_y^2. \quad (38)$$

The latter approximation in (38) is valid if $1/L_0 \ll k_y \ll \kappa$, i.e., the instability develops in the domain of wavelengths, which are larger than the ionization front thickness and smaller than the collisional ionization length. The magnetic field perturbation and the collisional ionization play stabilizing roles. The electrostatic assumption in (26) is verified if the parameter D, estimated in Eq. (12), is small.

The ionization instability described above is of the same nature as was derived recently in Ref. [10]. However, the stabilizing role of the collisional ionization and the magnetic field perturbations was not considered there. In the laboratory reference frame, the instability is convective, since it moves with the front at the velocity v_f. Indeed, the perturbations in the linear regime are of the form $\exp(ik'_x x' - i\omega' t')$. As the phase in the exponential is invariant, it is written

$$ik_x x - i\omega t \approx k_y\gamma_f(x - v_f t) + \frac{|\omega'|}{\gamma_f}t. \quad (39)$$

Thus, the instability growth rate in the laboratory reference frame is $|\omega| = |\omega'|/\gamma_f$, and the perturbation is attached to the beam head. Behind the front, the perturbation decreases with time. This result is consistent with the evanescent condition in the front reference frame.

The dependence of the instability growth rate, in the laboratory reference frame, on the beam and target characteristics is plotted in Fig. 3 for the typical parameters of present day experiments. It increases with the beam density, which is consistent with the qualitative description presented in the beginning of Sec. III. The growth rate weakly depends on the beam energy, however, the hypothesis of the nonrelativistic fast electrons in the front reference frame is restricted by a maximum beam energy of several tens of MeV, according to Eq. (13). Concerning the dependence on target characteristics, the instability growth rate increases with the ionization

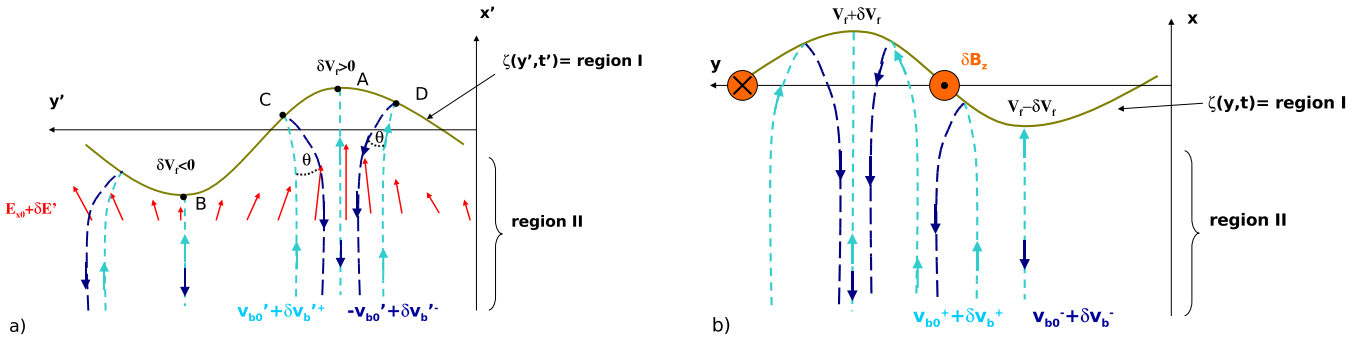

FIG. 4. (Color online) (a) Mechanism of the electric-field-driven ionization instability in the front reference frame. The beam front is symbolized by the green solid line. Behind the perturbed beam front, in region II, the electric field $\mathbf{E}_r' + \delta\mathbf{E}'$ is represented by red arrows, the fast electrons entering the front with the velocity $v_{b0}' + \delta\mathbf{v}_b'^{+}$ are shown with light blue dashed lines, and the fast electrons leaving the front with the velocity $-v_{b0}' + \delta\mathbf{v}_b'^{-}$ are shown with dark blue long dashed lines. (b) Mechanism of the ionization resistive instability in the laboratory reference frame. Two circles with the dot and the cross show the positive and negative magnetic field, respectively. The other symbols are the same as in (a).

potential, according to the formula $|\omega| \propto \Delta x_f' D \propto J_a^3$. Qualitatively, the beam corrugates faster as more energy is required to locally ionize the matter. The instability growth rate weakly depends on the target density, which is consistent with our assumption of a weak field ionization, $n_i \ll n_a$.

1. Interpretation of the instability

In order to demonstrate the instability mechanism, we explicitly relate the beam characteristics with the front displacement in the front reference frame, by using the expressions for the growth rate (38) and the parallel wave number k_x' (35). The fast electron trajectories are schematically represented in Fig. 4(a). The front displacement $\zeta_0 \cos k_y y e^{-i\omega' t'}$ is defined by the relation $\partial_{t'}\zeta = \gamma_f^2 \delta v_f$. It is symbolized by the dark green solid line in Fig. 4(a). Let us assume a positive local perturbation of the beam density $\delta n_b'^{+}$. According to the condition Eq. (36), the electric field ionization is enhanced and the interface is accelerated. Consequently, the mean fast electron velocity, and therefore the fast electron current are increased. As the instability evolves at a low frequency, the current is neutralized and the return current also increases. Thus, the perturbation of the resistive longitudinal electric field is enhanced and is written

$$\frac{\delta E_x}{E_r} = 3\Delta x_f' k_y^2 \zeta_0 \cos k_y y e^{|\omega'|t' + k_y x'}. \tag{40}$$

The Faraday equation (26) provides the relation between the components of the electric field, $\delta E_y' = i\delta E_x$, and for the y component of the electric field:

$$\frac{\delta E_y'}{E_r} = -3\Delta x_f' k_y^2 \zeta_0 \sin k_y y e^{|\omega'|t' + k_y x'}. \tag{41}$$

The resistive electric field, represented by the red vectors in Fig. 4(a), points toward the high front velocity regions. Then, the fast electron trajectories are perturbed by the electric field according to Eqs. (29):

$$\frac{\delta \mathbf{v}_b'^{\pm}}{v_{b0}'} = \frac{1}{3\Delta x_f' k_y^2 v_{b0}'} (\mp k_y v_{b0}' + |\omega'|) \frac{\delta \mathbf{E}'}{E_r}. \tag{42}$$

Two forces acting on the fast electrons play role in the instability. First, the fast electrons, which come from the beam body with the velocity $v_{b0}' + \delta v_b'^{+}$ [light blue dashed lines in Fig. 4(a)], are deflected towards the valleys of the front corrugation by the transverse electrostatic field. When reaching the beam front, they are reflected by the strong electric field with the angle $\theta = (\delta v_b'^{+} + \delta v_b'^{-})/v_{b0}' \propto \sin k_y y$, normal to the beam head surface. In the hill and the valley of the front corrugation, points A and B, respectively, the angle is equal to zero, while it is positive at the point C and negative at the point D. Thus, in these two latter cases, the fast electrons are reflected towards the hill of the corrugation (dark blue solid lines). Then, the local beam density $\delta n_b'^{-}$ and the current density increase. This effect amplifies the return current that strenghtens the resistive electric field. Second, the electrons faster than the front are slown down by the longitudinal electrostatic field in the hill of the corrugated front (behind point A), while those coming in the region behind the valley (point B) are accelerated. Consequently, the local charge density $\delta n_b'^{+}$ in the hill front corrugation is increased, while it is decreased in the valley front corrugation. This effect can be clearly seen when inspecting the reflection condition (36):

$$\frac{\delta n_b'^{+} + \delta n_{b0}'^{-}}{2n_{b0}'} = 3\Delta x_f' k_y^2 \zeta_0 \cos k_y y e^{|\omega'|t' + k_y x'}. \tag{43}$$

The beam density perturbations are in the phase with the front displacement, thus, the front corrugation amplitude increases. This is a positive feedback, which strengthens the perturbation and corresponds to an unstable front evolution. In the nonlinear regime, it could lead to a full beam filamentation as the fast electrons preferentially propagate in higher conducting target regions where the return current losses are smaller.

In the laboratory reference frame, according the discussion after the expression (32), the transverse electric field δE_y is equal to zero and the magnetic field is transformed into $\delta B_z = -\delta E_y'/\gamma_f v_f$. Thus, in the laboratory reference

frame, the deflection of the fast electrons is due to the magnetic field, which is generated by the longitudinal electric field moving with the ionization front. This effect is described by the displacement current in the Ampère equation, $c^2 \mathrm{curl}\mathbf{B} = \partial_t \mathbf{E}$. For higher beam energies, the transverse Lorentz force $\delta F_y = -ev_{b0}\delta E'_y/\gamma_f v_f$ decreases and the longitudinal fast electron inertia increases. Consequently, the fast electron deflection is reduced, which, in turn, decreases the instability growth rate. Thus, although our present model is restricted to electron energies smaller than a few tens of MeV, a slower instability is expected for higher energies.

We can estimate the beam propagation distance required for the instability excitation assuming that the instability becomes visible for an amplification factor $\exp|\omega|t \sim 10$. For a beam with an electron energy of 500 keV and a current density of 450 A $\mu\mathrm{m}^{-2}$ propagating through a dielectric target with the ionization potential of 7 eV, the instability with the wavelength $\lambda = 1$ μm is excited after the propagation distance $L_i = 2v_f/|\omega| \sim 300$ μm. This length is larger than the characteristic length of the filament development observed in the experiments [5–7] (~ 100 μm). Moreover, the perturbation wavelength predicted by the model is one order of magnitude smaller than that seen in the experiments, where $\lambda \approx 10$ μm.

In addition to this electrostatic and a relatively slow instability, $|\omega| \sim 1$ ps^{-1}, localized near the ionization front, $|k'_x| \sim k_y$, the dispersion equation has another unstable branch, which corresponds to perturbations that penetrate deeply in the beam, $|k'_x| \ll k_y$. It is related to the magnetic field perturbations and the beam filamentation.

C. The ionization-resistive instability

The propagation of a relativistic electron beam in a weakly conducting homogeneous plasma gives rise to the filamentation instability [14,15]. There, the wave vector k_y is perpendicular to the direction of the beam propagation, and the perturbations do not depend on the x coordinate, $k'_x \to 0$. Here we will demonstrate that the perturbations of the ionization front are coupled to the magnetic field perturbations and may excite the resistive filamentation instability.

We consider the stability problem in the WKB approximation, assuming now that k'_x is small compared to ω'/v'_{b0}, but still the condition $k'_x L_0 \gg 1$ is verified. The Ampère equation (22) takes the following form:

$$-ik_y \frac{Q}{\kappa}\frac{v_f \delta B'_z}{E_r} = \frac{\delta n_b'^{+} + \delta n_b'^{-}}{2n'_{b0}} - \frac{\delta n'_i}{n'_{i0}} - \frac{\delta E_x}{E_r} + \frac{v'_{b0}}{v_f}\frac{\delta v_{bx}'^{+} + \delta v_{bx}'^{-}}{2v'_{b0}}, \tag{44}$$

where the contribution of the fast electron density perturbation is neglected because of a small electron velocity, $v'_{b0} \ll v_f$, and the charge neutralization condition (20). The plasma charge continuity equation (23) can be simplified by taking into account the quasineutrality condition:

$$\left(\frac{\omega'}{v_f} + k'_x\right)\frac{\delta n_b'^{+} + \delta n_b'^{-}}{2n'_{b0}} = k'_x\left(\frac{\delta n'_i}{n'_{i0}} + \frac{\delta E_x}{E_r}\right) + k_y\gamma_f^2\frac{\delta E'_y + v_f \delta B'_z}{E_r}. \tag{45}$$

It is complemented with the ionization equation

$$\left(\frac{\omega'}{v_f} + k'_x\right)\frac{\delta n'_i}{n'_{i0}} \approx \frac{2i}{L_0}\frac{\delta E_x}{E_r}. \tag{46}$$

The total beam charge density and the total longitudinal beam velocity follow from Eqs. (17) and (19). In the limit $\omega' \gg k'_x v'_{b0}$ one finds

$$\frac{\delta n_b'^{+} + \delta n_b'^{-}}{2n'_{b0}} \approx -\frac{i\kappa v_{b0}'^2}{\omega'^2}\frac{k'_x \delta E_x + k_y \delta E'_y}{E_r}, \tag{47}$$

$$\frac{\delta v_{bx}'^{+} + \delta v_{bx}'^{-}}{2v'_{b0}} \approx -\frac{i\kappa v'_{b0}}{\omega'}\frac{\delta E_x}{E_r}. \tag{48}$$

The Faraday equation (21) closes this system of equations for the perturbations.

1. Resistive instability, case $k'_x = 0$

It is instructive first to consider the case of a homogeneous beam and a perturbation in the limit $k'_x = 0$. In this case Eq. (46) gives $\delta n'_i = 0$ and the rest of equations can be reduced to the dispersion relation

$$\left(Q - i\frac{\omega'\kappa}{k_y^2 v_f} + \frac{\kappa^2 v_{b0}'^2}{k_y^2 v_f^2}\right)\left(1 + i\frac{\kappa v_{b0}'^2}{\omega' v_f \gamma_f^2}\right) = -\frac{\kappa^2 v_{b0}'^2}{\omega'^2}. \tag{49}$$

In the limit $\delta E'_y \sim -v_f \delta B'_z$, *i.e.* $\omega' \gg \kappa v_{b0}'^2/v_f\gamma_f^2$, according to Eq. (45), this equation can be written in the form

$$R(\omega', k_y) = i\frac{\sigma_{\min}}{\gamma_f \varepsilon_0 \omega'_{b0}}\frac{\omega'^3}{\omega_{b0}'^3} - \left(1 + \frac{k_y^2 c^2}{\omega_{b0}'^2}\right)\frac{\omega'^2}{\omega_{b0}'^2} - \frac{k_y^2 v_f^2}{\omega_{b0}'^2} = 0, \tag{50}$$

where $\omega'_{b0} = \sqrt{2e^2 n'_{b0}/m\varepsilon_0}$ is the fast electron plasma frequency in the front reference frame. This equation is equivalent to the dispersion equation introduced in Ref. [15] in the laboratory reference frame. For sufficiently high wave numbers, $k_y \gg \kappa(v'_{b0}/v_f)^{1/2}Q^{3/4}$, this equation has a solution corresponding to an instability: $\omega' \approx i\kappa v'_{b0}/Q^{1/2} = \omega'_{b0}v_f/c$. This growth rate, which is of the order of the beam plasma frequency, is consistent with the fact that the fast electrons perturbation cannot grow faster than their characteristic betatron time. For the smaller wavelengths, $\varepsilon_0\gamma_f\omega_{b0}'^2/\sigma_{\min}v_f \ll k_y \ll \omega'_{b0}/c$, the growth rate takes the form $\omega' = (\varepsilon_0\gamma_f\omega_{b0}'^2 v_f^2 k_y^2/\sigma_{\min})^{1/3}$, as is shown in the Appendix. This solution is consistent with the assumption $\omega' \gg \kappa v_{b0}'^2/v_f\gamma_f^2$, which corresponds to the wave numbers $k_y \gg \varepsilon_0\omega_{b0}'^2/\sigma_{\min}v_f\gamma_f^2$. The return current is not deflected as $\delta E'_y + v_f\delta B'_z = 0$, which agrees with the assumption $\delta E_y = 0$ made in Ref. [15].

2. Ionization resistive instability, case $k'_x v'_{b0} \ll \omega'$, $k'_x \ll k_y$

Let us consider now the effect of the ionization front on this instability, assuming that $k'_x \ll k_y$. One can construct the characteristic equation for the parallel wave number k'_x from the system (21) and (44)–(48) by applying the simplifying hypotheses that we have verified in the limit $k'_x = 0$. Accordingly, we limit ourselves to the first order expansion in k'_x and the continuity equation (45) can be simplified to $\delta E'_y =$

$-v_f \delta B_z'$. The longitudinal field variation is set up by the Faraday law (21), i.e. $k_y \delta E_x = (\omega'/v_f + k_x')\delta E_y'$. Then, the last equation (44) coupled to the ionization equation (46) and the total beam velocity equation (48) provides the characteristic equation

$$-i\frac{\omega'^2 v_f^2}{\omega_{b0}'^2 v_{b0}'^2 \kappa} k_x' = R(\omega', k_y) - \frac{2}{L_0 \kappa}\frac{v_f^2}{v_{b0}'^2}\frac{\omega'^2}{\omega_{b0}'^2}. \tag{51}$$

It reduces to the dispersion equation for the dissipative instability of a semi-infinite electron beam in the limit $\kappa \to \infty$, which corresponds to the infinitely thin ionization layer. Since the longitudinal wave number k_x' is assumed to be larger than $1/L_0$, the right-hand term proportional to $1/L_0\kappa$ in Eq. (51) can be considered as a perturbation. Knowing the longitudinal wave number, one can use the boundary condition (36) to find the dispersion equation

$$k_x' + \frac{\omega'}{v_f} = 2\gamma_f^2 D \frac{v_f k_y^2}{\omega'}. \tag{52}$$

Excluding the parallel wave number from these two equations we obtain finally the dispersion equation for the frequency ω' in function of k_y:

$$\frac{v_{b0}'^2 k_y^2}{\omega'^2} + \frac{Q k_y^2}{\kappa^2} = -\frac{2}{L_0 \kappa} + 2i\gamma_f^2 D \frac{v_f k_y^2}{\omega' \kappa}. \tag{53}$$

The conductivity does not appear in this dispersion equation because, in the electric field ionization model, it is defined by the beam characteristics, and hence, it does not act as an independent parameter. Without the collisional ionization term $2/L_0\kappa$, two limits are rather evident. In the case of the fast ionization wave, where, $D v_f / v_{b0}' \ll 1$, the electric field ionization effect is not important and the resistive instability dominates. It is described by the left hand terms in Eq. (53). In the contrary, for the case where $\gamma_f^2 D v_f / v_{b0}' \gg 1$, the ionization front enhances the growth rate, $\omega' \approx 2i\gamma_f^2 D \kappa v_f / Q$. Taking into account the collisional ionization term, the solution of the dispersion equation (53) can be presented in two asymptotic forms:

$$\mathrm{Im}\,\omega' = \begin{cases} \omega_{b0}' \dfrac{v_f}{c}\left(1 + \gamma_f^2 D \dfrac{c\kappa}{Q\omega_{b0}'} - \dfrac{1}{L_0}\dfrac{\kappa}{k_y^2 Q}\right) & \text{for } \gamma_f^2 D \dfrac{v_f}{v_{b0}'} \ll 1, \quad (54) \\ 2\gamma_f^2 \dfrac{D}{Q}\kappa v_f \left(1 - \dfrac{2}{L_0}\dfrac{\kappa}{Q k_y^2}\right) & \text{for } \gamma_f^2 D \dfrac{v_f}{v_{b0}'} \gg 1. \quad (55) \end{cases}$$

As in the case of the electrostatic instability presented in Sec. III B, the collisional ionization decreases the instability growth rate. This effect is amplified for small wave numbers. For beam parameters of present day experiments, the criterion $\gamma_f^2 D v_f / v_{b0}' \ll 1$ is valid and the growth rate is defined by Eq. (54). The growth rate in the laboratory reference frame is plotted in Fig. 5 in the domain of validity of the model, that is, $\sqrt{\kappa/L_0} \ll k_y \ll \kappa$. In the limit of high wave numbers, the instability growth rate saturates at the beam plasma frequency $\mathrm{Im}\,\omega = \omega_{b0} v_f / c \gamma_f^{3/2}(1 + \gamma_f^2 D \kappa c / Q \omega_{b0}')$. It is not sensitive to the target ionization potential, contrary to the electrostatic instability.

It is convenient to describe the ionization-resistive instability mechanism in the laboratory reference frame [see the scheme presented in Fig. 4(b)]. Let us assume a positive perturbation of the incoming electron density, δn_b^+. The electric field ionization is enhanced and the beam front velocity increases as well as the mean fast electron velocity. The fast electron current density is amplified and, since the instability occurs at a high frequency, the return current does not neutralize the incident beam, consequently a focusing magnetic field is generated (two orange circle symbols, with a dot for the positive magnetic field, and a cross for the negative one).

The fast electrons moving with the velocity v_{b0}^+ (light blue long dashed lines) are deflected by the transverse electric field towards the hill. They are reflected at the ionization front and move slower than it with the velocity v_{b0}^- (dark blue dashed lines), where $v_{b0} \sim 2vf - v_{b0}$. Consequently, the total fast electron density δn_b increases behind the hill, while it decreases behind the valley. The ionization in the front becomes more efficient, the front is accelerated. This provides a positive feedback for the instability.

Compared to the classical resistive instability, the ionization resistive instability corresponds to the high-frequency regime, where the beam pinch effect is dominant. This latter is amplified by the corrugation of the ionization front due to the electric field ionization.

The growth rate is proportional to the square root of the beam density and inversely proportional to $\gamma_{b0}^{3/2}$. For a beam current density of 450 A $\mu\mathrm{m}^{-2}$ and for the electrons with an energy of 500 keV, the perturbation growth rate at the wavelength of $\lambda = 1$ μm can be estimated as $\mathrm{Im}\,\omega \simeq 10^{13}$ s^{-1}. In the laboratory reference frame, according to the discussion of Sec. III B, the instability is convective and the front corrugation occurs very quickly, after several tens of μm of propagation. The growth rate for high wavelengths can be found for sufficiently high beam energies. A beam with a current density of 450 A $\mu\mathrm{m}^{-2}$ and an energy of 5 MeV corrugates on the distance of $L_i = 2v_f/|\omega| \sim 300$ μm for a perturbation wavelength of $\lambda = 6$ μm. Similarly to the electric field

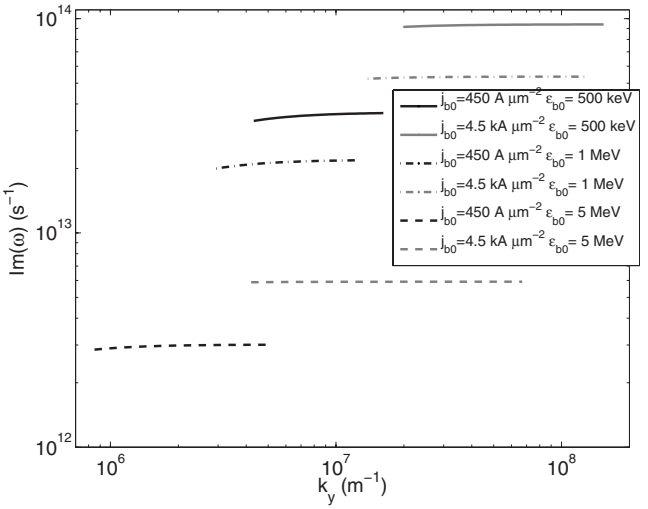

FIG. 5. Dependence of the ionization resistive instability growth rate Im ω on the transverse wave number k_y for different beam energies and beam current densities. The parameters are the same as presented in Fig. 3(a).

driven instability, the model is not valid for higher wavelengths. However our analysis shows that this electromagnetic instability is dominant for small perturbation size of the order of 1 μm.

IV. CONCLUSION

We analyzed here the stability of a monoenergetic fast electron beam propagation through a dielectric target. The particularity of the fast electron propagation in a dielectric target is due to the electric field ionization that takes place in a narrow region in the beam head. It provides the return plasma electron current, which continues the ionization process by electron-atom collisions. The fast electrons are slowed down in the electric field ionization region. These two populations of fast electrons, incoming ones and slowed down ones, play an important role in the instability mechanism.

Assuming that the perturbation wavelengths are larger than the electric field ionization front thickness, two instabilities are found.

In the low-frequency regime, the corrugation of the front increases the fast electron current. Then, the return current is increased and it amplifies the electrostatic field. This latter creates a magnetic field because this electric field is moving with the ionization front. Two effects are driving the instability. First, the specular reflection of the fast electrons in the ionization front and their concentration in the high front velocity region by the magnetic field, reinforce the return current and thus amplify the resistive electric field. Second, the longitudinal electric field, which is higher behind the high front velocity region, concentrates the fast electrons entering the front that amplifies the front corrugation. The fast electron current increases and that provides the instability feedback. The instability occurs near the beam head. Its growth rate is relatively weak, $\sim 10^{12}-10^{13}$ s^{-1} and depends strongly on the target ionization potential. For instance, in a beam with a current density of $j_b \sim 450$ A μm^{-2} and a mean electron energy of $\epsilon_b = 500$ keV, the front corrugation with a size of 0.6 μm appears after a propagation over 100 μm for a target ionization potential of 7 eV. This amplification length agrees with the observations [4,5,7–9], however for the filaments of ten times smaller size.

In the high-frequency regime, the instability is driven by the magnetic field. It is similar to the pinch effect of the resistive instability [14,15], but it is amplified by the front corrugation due to the beam density perturbation. The corrugation of the ionization front increases the fast electron current and amplifies the magnetic field. The fast electrons are deflected by the magnetic field toward the high beam density region, which locally enhances the electric field ionization in the front. The front corrugation is amplified, which makes a positive feedback for the instability. The growth rates of this instability are more than an order of magnitude higher than those of the electrostatic instability. However, due to the restricted domain of validity of the model, our analytical calculations are limited to sufficiently high beam energies or high beam densities. For a beam with a current density of 450 A μm^{-2} and an electron energy of 5 MeV, the front corrugates into filaments of 5 μm in diameter after one hundred μm of propagation. For a lower mean electron energy of 1 MeV, the beam front corrugation with the size of $\lambda \approx 1$ μm appears very quickly after 30 μm of propagation. This instability develops faster compared to the electric field driven instability. However, due to the collisional ionization which increases the plasma electron density, this instability is restricted to relatively short wavelengths. Thus, although the predicted growth rate is comparable with the numerical simulations and observations [16–19], this instability cannot explain the large scale beam filamentation ($\lambda \sim 10$ μm).

The electric-field-driven instability decreases for higher beam densities and it does not depend on the beam energy. The ionization-resistive instability increases with the beam density and is strongly reduced for higher mean electron energies. However, in both cases, for a given instability growth rate, the higher the beam density, the smaller the characteristic perturbation wavelength.

Several other effects, which have not been studied here, could modify the instability characteristics. First, in our monoenergetic fast electron model, all incoming fast electrons penetrate the ionization front since they are all moving at a velocity v_{b0} higher than the front velocity v_f. A more realistic fast electron distribution function may modify the beam front velocity dependence on the beam density, since, only the fastest electrons in the beam would contribute to the electric field ionization in the front. Second, our present theory is valid in the WKB approximation, which assumes a weak collisional ionization. A more detailed, quantitative analysis is needed for calculating the growth rates for smaller wave numbers and smaller beam currents.

APPENDIX

The resistive filamentation of an electron current is due to the fast electron deviation in the electric and magnetic field created by a return electron current. Its growth rate depends

on the plasma resistivity. This instability was considered in Refs. [14,15] in the laboratory frame. We demonstrate here how this instability can be described in the front reference frame. Similarly to the initial condition of Ref. [15], we assume a full plasma charge neutralization and identify the frame velocity with the velocity of a monoenergetic electron beam. Then the dispersion equation for the resistive filamentation instability reads:

$$i\frac{\sigma_{\min}}{\gamma_f \varepsilon_0 \omega'_{b0}}\frac{\omega'^3}{\omega'^3_{b0}} - \left(1 + \frac{k_y^2 c^2}{\omega'^2_{b0}}\right)\frac{\omega'^2}{\omega'^2_{b0}} - \frac{k_y^2 v_f^2}{\omega'^2_{b0}} = 0, \qquad \text{(A1)}$$

where $\sigma_{\min} = e^2 n_{i\,\max}/m\nu_e$ is the electrical plasma conductivity introduced in Sec. II B.

Note that this equation differs from the one presented in Ref. [15] as the perturbation of the conductivity, $\delta\sigma' E_r \propto k_y'^2 v_f^2/\omega'^2_{b0}$, is not negligible in the front reference frame. In the limit of long wavelengths, $k_y c \ll \omega'_{b0}$, one has

$$i\omega'^3 = \frac{\varepsilon_0 \gamma_f \omega'^2_{b0}}{\sigma_{\min}}(\omega'^2 + k_y^2 v_f^2). \qquad \text{(A2)}$$

Considering also the case of low frequencies, $\omega' \ll k_y v_f$, we find the instable root

$$\omega' = \left(\frac{\varepsilon_0 \gamma_f \omega'^2_{b0} k_y^2 v_f^2}{\sigma_{\min}}\right)^{1/3}, \qquad \text{(A3)}$$

which is valid as long as $\varepsilon_0 \gamma_f \omega'^2_{b0}/\sigma_{\min} v_f \ll k_y \ll \omega'_{b0}/c$.

[1] K. B. Wharton, S. P. Hatchett, S. C. Wilks, M. H. Key, J. D. Moody, V. Yanovsky, A. A. Offenberger, B. A. Hammel, M. D. Perry, and C. Joshi, Phys. Rev. Lett. **81**, 822 (1998).

[2] J. J. Santos *et al.*, Phys. Rev. Lett. **89**, 025001 (2002).

[3] E. Martinolli, M. Koenig, F. Amiranoff, S. D. Baton, L. Gremillet, J. J. Santos, T. A. Hall, M. Rabec-Le-Gloahec, C. Rousseaux, and D. Batani, Phys. Rev. E **70**, 055402(R) (2004).

[4] J. Fuchs *et al.*, Phys. Rev. Lett. **91**, 255002 (2003).

[5] M. Manclossi, J. J. Santos, D. Batani, J. Faure, A. Debayle, V. T. Tikhonchuk, and V. Malka, Phys. Rev. Lett. **96**, 125002 (2006).

[6] M. Borghesi, A. J. MacKinnon, A. R. Bell, G. Malka, C. Vickers, O. Willi, J. R. Davies, A. Pukhov, and J. Meyer-ter-Vehn, Phys. Rev. Lett. **83**, 4309 (1999).

[7] L. Gremillet *et al.*, Phys. Rev. Lett. **83**, 5015 (1999).

[8] M. Tatarakis *et al.*, Phys. Rev. Lett. **90**, 175001 (2003).

[9] R. B. Stephens *et al.*, Phys. Rev. E **69**, 066414 (2004).

[10] S. I. Krasheninnikov, A. V. Kim, B. K. Frolov, and R. Stephens, Phys. Plasmas **12**, 073105 (2005).

[11] A. Debayle and V. T. Tikhonchuk, Phys. Plasmas **14**, 073104 (2007).

[12] O. Klimo, V. T. Tikhonchuk, and A. Debayle, Phys. Rev. E **75**, 016403 (2007).

[13] Y. Zel'dovich and Y. Raizer, *Physics of Shock Waves and High-Temperature Hydrodynamic Phenomena* (Dover, New York, 2002), pp. 387–412.

[14] Yu. M. Aliev, V. Yu. Bychenkov, and A. A. Frolov, Phys. Fluids **25**, 827 (1983).

[15] L. Gremillet, G. Bonnaud, and F. Amiranoff, Phys. Plasmas **9**, 941 (2002).

[16] S. C. Wilks, W. L. Kruer, M. Tabak, and A. B. Langdon, Phys. Rev. Lett. **69**, 1383 (1992).

[17] F. N. Beg, A. R. Bell, A. E. Dangor, C. N. Danson, A. P. Fews, M. E. Glinsky, B. A. Hammel, P. Lee, P. A. Norreys, and M. Tatarakis, Phys. Plasmas **4**, 447 (1996).

[18] M. Chen, Z.-M. Sheng, and J. Zhang, Phys. Plasmas **13**, 014504 (2006).

[19] C. I. Moore, J. P. Knauer, and D. D. Meyerhofer, Phys. Rev. Lett. **74**, 2439 (1995).